

Improved Singular Spectrum Analysis for Time Series with Missing Data

Y. Shen¹ F. Peng^{1,2} B. Li¹

1. College of Surveying and Geo-informatics, Tongji University, Shanghai, PR, China
2. Center for Spatial Information Science and Sustainable Development, Shanghai, PR, China

Abstract. Singular spectrum analysis (SSA) is a powerful technique for time series analysis. Based on the property that the original time series can be reproduced from its principal components, this contribution develops an improved SSA (ISSA) for processing the incomplete time series and the modified SSA (SSAM) of Schoellhamer (2001) is its special case. The approach is evaluated with the synthetic and real incomplete time series data of suspended-sediment concentration from San Francisco Bay. The result from the synthetic time series with missing data shows that the relative errors of the principal components reconstructed by ISSA are much smaller than those reconstructed by SSAM. Moreover, when the percentage of the missing data over the whole time series reaches 60%, the improvements of relative errors are up to 19.64, 41.34, 23.27 and 50.30% for the first four principal components, respectively. Besides, both the mean absolute error and mean root mean squared error of the reconstructed time series by ISSA are also smaller than those by SSAM. The respective improvements are 34.45 and 33.91% when the missing data accounts for 60%. The results from real incomplete time series also show that the standard deviation (SD) derived by ISSA is 12.27mg L⁻¹, smaller than 13.48 mg L⁻¹ derived by SSAM.

Keywords: Time series analysis, Singular spectrum Analysis, Missing Data

1. Introduction

Singular spectrum analysis (SSA) introduced by Broomhead and King (1986) for studying dynamical systems is a powerful toolkit for extracting short, noisy and chaotic signals (Vautard et al., 1992). SSA first transfers a time series into trajectory matrix, and carries out the principal component analysis to pick out the dominant components of the trajectory matrix. Based on these dominant components, the time series is reconstructed. Therefore the reconstructed time series improves the signal to noise ratio and reveals the characteristics of the original time series. SSA has been widely used in geosciences to analyze a variety of time series, such as the stream flow and sea-surface temperature (Robertson and Mechoso, 1998; Kondrashov and Ghil, 2006), the seismic tomography (Oropeza and Sacchi, 2011) and the monthly gravity field (Zotova and Shum, 2010). Schoellhamer (2001) developed a modified SSA for time series with missing data (SSAM), which was successfully applied to analyze the time series of suspended-sediment concentration (SSC) in San Francisco Bay (Schoellhamer, 2002). This SSAM approach doesn't need to fill missing data. Instead, it computes the each principal component (PC) with observed data and a scale factor related to the number of missing data. Shen et al. (2014) developed a new principal component analysis approach for extracting common mode errors from the

43 time series with missing data of a regional station network. The other kind of SSA
 44 approaches process the time series with missing data by filling the data gaps
 45 recursively or iteratively, such as the ‘‘Catterpillar’’-SSA method (Golyandina and
 46 Osipov, 2007), the imputation method (Rodrigues and Carvalho, 2013) or the iterative
 47 method (Kondrashov and Ghil, 2006).

48 This paper is motivated by Schoellhamer (2001) and Shen et al. (2014) and develops
 49 an improved SSA (ISSA) approach. In our ISSA, the lagged correlation matrix is
 50 computed with the same way as Schoellhamer (2001), the PCs are directly computed
 51 with both the eigenvalues and eigenvectors of the lagged correlation matrix. However,
 52 the PCs in Schoellhamer (2001) were calculated with the eigenvectors and a scale
 53 factor to compensate the missing value. Moreover, we do not need to fill the missing
 54 data recursively and iteratively as in Golyandina and Osipov (2007). The rest of this
 55 paper is organized as follows: the improvement of SSA for time series with missing
 56 data will be followed in Sect. 2, synthetic and real numerical examples are presented
 57 in Sects. 3 and 4 respectively, and then conclusions are given in last Sect. 5.

58 2. Improved Singular Spectrum Analysis for Time Series with Missing Data

59 For a stationary time series x_i ($1 \leq i \leq N$), we can construct an $L \times (N-L+1)$ trajectory
 60 matrix with a window size L , its Toeplitz lagged correlation matrix \mathbf{C} is formulated by

$$61 \quad \mathbf{C} = \begin{bmatrix} c(0) & c(1) & \cdots & c(L-1) \\ c(1) & c(0) & \ddots & \vdots \\ \vdots & \vdots & \ddots & c(1) \\ c(L-1) & \cdots & \cdots & c(0) \end{bmatrix} \quad (1)$$

62 Each element $c(j)$ is computed by

$$63 \quad c(j) = \frac{1}{N-j} \sum_{i=1}^{N-j} x_i x_{i+j} \quad j = 0, 1, 2, \dots, L-1 \quad (2)$$

64 For matrix \mathbf{C} , we can compute its eigenvalues λ_k and the corresponding eigenvectors
 65 \mathbf{v}_k in descending order of λ_k ($1 \leq k \leq L$). Then the i th element of k th principal
 66 components (PCs) \mathbf{a}_k is computed by

$$67 \quad a_{k,i} = \sum_{j=1}^L x_{i+j-1} v_{j,k} \quad 1 \leq i \leq N-L+1 \quad (3)$$

68 where $v_{j,k}$ is the j th element of \mathbf{v}_k . We compute the k th reconstructed components
 69 (RCs) of the time series with the k th PCs as (Vautard et al., 1992)

$$70 \quad x_i^k = \begin{cases} \frac{1}{i} \sum_{j=1}^i a_{k,i-j+1} v_{j,k} & 1 \leq i \leq L-1 \\ \frac{1}{L} \sum_{j=1}^L a_{k,i-j+1} v_{j,k} & L \leq i \leq N-L+1 \\ \frac{1}{N-i+1} \sum_{j=i-N+L}^L a_{k,i-j+1} v_{j,k} & N-L+2 \leq i \leq N \end{cases} \quad (4)$$

71 Since λ_k , the variance of the k th RC, is sorted in descending order, the first several
 72 RCs contain most of the signals of the time series, while the remaining RCs contain
 73 mainly the noises of time series. Thus the original time series is reconstructed with
 74 first several RCs.

75 The SSAM approach developed by Schoellhamer (2001) computes the elements $c(j)$
 76 of the lagged correlation matrix by,

$$77 \quad c(j) = \frac{1}{N_j} \sum_{i \leq N-j} x_i x_{i+j} \quad j = 0, 1, 2, \dots, L-1 \quad (5)$$

78 where, both x_i and x_{i+j} must be observed rather than missed, N_j is the number of the
 79 products of x_i and x_{i+j} within the sample index $i \leq N-j$. Then we compute the
 80 eigenvalues and eigenvectors from the lagged correlation matrix C . The PCs are also
 81 calculated with observed data,

$$82 \quad a_{k,i} = \frac{L}{L_i} \sum_{1 \leq j \leq L} x_{i+j-1} v_{j,k} \quad 1 \leq i \leq N-L+1 \quad (6)$$

83 where L_i is the number of observed data within the sample index from i to $i+L-1$. The
 84 reconstruction procedure of time series from PCs is the same as SSA. The scale factor
 85 L/L_i is used to compensate the missing value.

86 In order to derive the expression of computing PCs for the time series with missing
 87 data, the Eq. (3) is reformulated as,

$$88 \quad a_{k,i} = \sum_{i+j-1 \in S_i} x_{i+j-1} v_{j,k} + \sum_{i+j-1 \in \bar{S}_i} x_{i+j-1} v_{j,k} \quad (7)$$

89 where, $1 \leq i \leq N-L+1$, S_i and \bar{S}_i are the index sets of sampling data and missing
 90 data respectively within the integer interval $[i, i+L-1]$, i.e. $S_i \cap \bar{S}_i = 0$ and
 91 $S_i \cup \bar{S}_i = [i, i+L-1]$. If PCs are available, we can reproduce the missing values. Therefore,
 92 the missing values in Eq. (7) can be substituted with PCs as,

$$93 \quad x_{i+j-1} = \sum_{m=1}^L a_{m,i} v_{j,m} \quad (8)$$

94 Substituting Eq. (8) into the second term of the right hand of Eq. (7) yields,

$$95 \quad \left(1 - \sum_{i+j-1 \in \bar{S}_i} v_{j,k}^2\right) a_{k,i} - \sum_{i+j-1 \in \bar{S}_i} \sum_{m=1, m \neq k}^L v_{j,m} v_{j,k} a_{m,i} = \sum_{i+j-1 \in S_i} x_{i+j-1} v_{j,k} \quad (9)$$

96 Collecting all equations of Eq. (9) for $k=1,2,\dots,L$, we have,

$$97 \quad \mathbf{G}_i \boldsymbol{\xi}_i = \mathbf{y}_i \quad (10)$$

98 where,

$$99 \quad \mathbf{G}_i = \begin{bmatrix} 1 - \sum_{i+j-1 \in \bar{S}_i} v_{j,1}^2 & - \sum_{i+j-1 \in \bar{S}_i} v_{j,1} v_{j,2} & \cdots & - \sum_{i+j-1 \in \bar{S}_i} v_{j,1} v_{j,L} \\ - \sum_{i+j-1 \in \bar{S}_i} v_{j,2} v_{j,1} & 1 - \sum_{i+j-1 \in \bar{S}_i} v_{j,2}^2 & \cdots & - \sum_{i+j-1 \in \bar{S}_i} v_{j,2} v_{j,L} \\ \vdots & \vdots & \ddots & \vdots \\ - \sum_{i+j-1 \in \bar{S}_i} v_{j,L} v_{j,1} & - \sum_{i+j-1 \in \bar{S}_i} v_{j,L} v_{j,2} & \cdots & 1 - \sum_{i+j-1 \in \bar{S}_i} v_{j,L}^2 \end{bmatrix}, \quad (11)$$

$$100 \quad \boldsymbol{\xi}_i = \begin{bmatrix} a_{1,i} \\ a_{2,i} \\ \vdots \\ a_{L,i} \end{bmatrix}, \quad \mathbf{y}_i = \begin{bmatrix} \sum_{i+j-1 \in S_i} x_{i+j-1} v_{j,1} \\ \sum_{i+j-1 \in S_i} x_{i+j-1} v_{j,2} \\ \vdots \\ \sum_{i+j-1 \in S_i} x_{i+j-1} v_{j,L} \end{bmatrix} \quad (12)$$

101 Since \mathbf{G}_i is a symmetric and rank-deficient matrix with the number of rank-deficiency
 102 equaling to the number of missing data within the interval $[x_i, x_{i+L-1}]$, the PCs $a_{k,i}$
 103 ($k=1, 2, \dots, L$) are solved with Eq. (10) based on the following criterion (Shen et al.
 104 2014),

$$105 \quad \min : \boldsymbol{\xi}_i^T \mathbf{A}^{-1} \boldsymbol{\xi}_i \quad (13)$$

106 where, \mathbf{A} is diagonal matrix of eigenvalues λ_k , which is the covariance matrix of PCs.
 107 The solution of Eq. (10) is as follows,

$$108 \quad \boldsymbol{\xi}_i = \mathbf{A} \mathbf{G}_i^T (\mathbf{G}_i^T \mathbf{A} \mathbf{G}_i)^{-} \mathbf{y}_i \quad (14)$$

109 The symbol ‘-’ denotes the pseudo-inverse of a matrix.

110 If the non-diagonal elements of \mathbf{G}_i are all set to zero, the Eq. (14) can be further
 111 simplified as,

$$112 \quad a_{k,i} = \frac{1}{1 - \sum_{i+j-1 \in \bar{S}_i} v_{k,j}^2} \sum_{1 \leq j \leq L} x_{i+j-1} v_{j,k} \quad 1 \leq k \leq L, 1 \leq i \leq N-L+1 \quad (15)$$

113 Supposing $v_{1,k} = v_{2,k} = \dots = v_{L,k} = 1/\sqrt{L}$ at the missing data points, the solution of Eq.
 114 (15) will be reduced to Eq. (6). Therefore, the SSAM approach is a special case of our
 115 ISSA approach. By the way, the first several PCs contain most variance; the element
 116 x_{i+j-1} can be approximately reproduced with the first several PCs in Eq. (8).

117 The main difference of our ISSA approach from the SSAM approach of Schoellhamer
 118 (2001) is in calculating the PCs. We produce the PCs from observed data with Eq. (14)
 119 according to the power spectrum (eigenvalues) and eigenvectors of the PCs. While
 120 Schoellhamer (2001) calculates the PCs from observed data with Eq. (6) only
 121 according to the eigenvectors and uses the scale factor L/L_i to compensate the missing
 122 value. We have pointed out that this scale factor can be derived from Eq. (15), which
 123 is the simplified version of our ISSA approach, by supposing the missing data points
 124 with the same eigenvector elements. Therefore the performance of our ISSA approach
 125 is better than SSAM of Schoellhamer (2001). The only disadvantage of our method is
 126 that it will cost more computational effort.

127 3. Performance of ISSA with synthetic time series

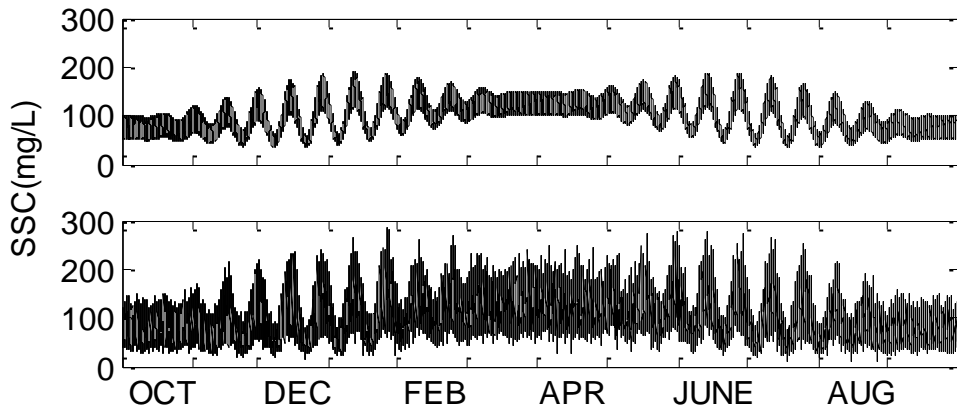
128 The same synthetic time series as Schoellhamer (2001) are used to analyze the
 129 performance of ISSA compared to SSAM. The synthetic SSC time series is expressed
 130 as,

$$131 \quad c(t) = 0.2R(t)c_s(t) + c_s(t) \quad (16)$$

132 where, $R(t)$ is a time series of Gaussian white noise with zero mean and unit standard
 133 deviation; $c_s(t)$ is the periodic signal expressed as,

$$134 \quad c_s(t) = 100 - 25 \cos \omega_s t + 25(1 - \cos 2\omega_s t) \sin \omega_{sn} t \\ + 25(1 + 0.25(1 - \cos 2\omega_s t) \sin \omega_{sn} t) \sin \omega_a t \quad (17)$$

135 The periodic signal oscillates about the mean value 100mg L^{-1} including the signals
 136 with seasonal frequency $\omega_s = 2\pi / 365 \text{ day}^{-1}$, spring/neap angular frequency
 137 $\omega_{sn} = 2\pi / 14 \text{ day}^{-1}$ and advection angular frequency $\omega_a = 2\pi / (12.5 / 24) \text{ day}^{-1}$. The one
 138 year of synthetic SSC time series $c(t)$, starting at October 1 with 15-minute time step,
 139 is presented on the bottom of Fig. 1, the corresponding periodic signal $c_s(t)$ is
 140 shown on the top of Fig. 1.



141
 142 Figure 1. periodic signal $c_s(t)$ (top) and Synthetic time series (bottom)

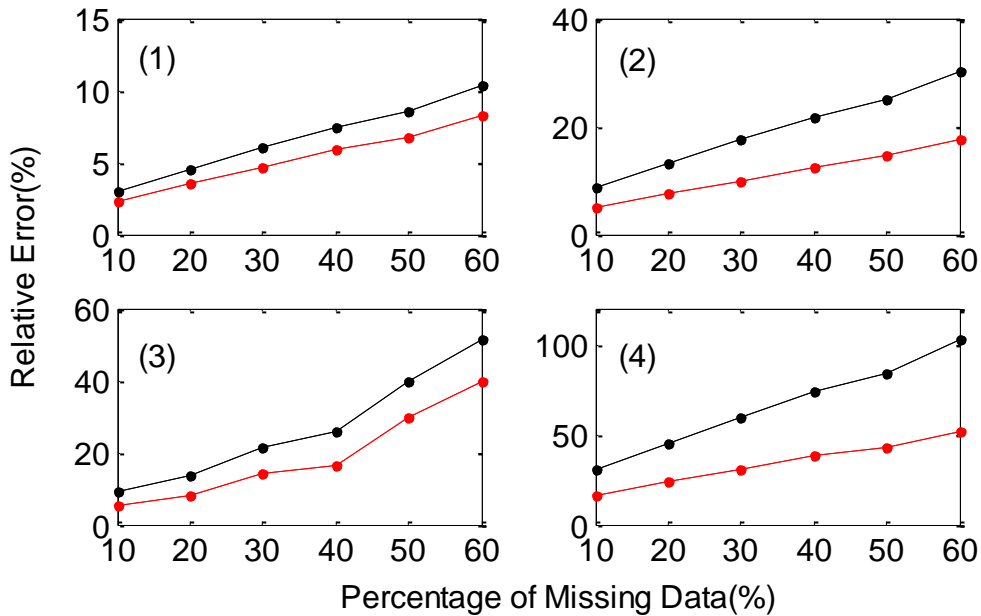
143 Although the selection of window length is an important issue for SSA (Hassani 2012,

144 2013), this paper chooses the same window length ($L=120$) as that in Schoellhamer
 145 (2001) in order to compare the performance of the proposed method with that of
 146 Schoellhamer (2001). Using the synthetic time series we compute the lagged
 147 correlation matrix and the variances of each mode. The first 4 modes contain the
 148 periodic components, which account for 72.3% of the total variance; particularly, the
 149 first mode contains 50.2% of the total variance. In order to evaluate the accuracies of
 150 reconstructed PCs from the time series with different percentages of missing data,
 151 following the way of Shen et al. (2014), we compute the relative errors of the first
 152 four modes derived by ISSA and SSAM with the following expression,

$$153 \quad p = \frac{1}{N} \sum_{i=1}^N \sqrt{\frac{(\mathbf{a}_i - \mathbf{a}_0)^T (\mathbf{a}_i - \mathbf{a}_0)}{\mathbf{a}_0^T \mathbf{a}_0}} \times 100\% \quad (18)$$

154 where, The symbol ‘ T ’ denotes the transpose of a matrix; p denotes relative error; N is
 155 the number of repeated experiments; \mathbf{a}_i is the reconstructed PCs of i th experiment
 156 from data missing time series, \mathbf{a}_0 denotes the PCs reconstructed from the time series
 157 without missing data. We design the experiment of missing data by randomly deleting
 158 the data from the synthetic time series. The percentage of deleted data is from 10% to
 159 60% with an increase of 10% each time. Then, we reconstruct the first four PCs from
 160 the data deleted synthetic time series using both SSAM and ISSA, and repeat the
 161 experiments for 50 times. The relative errors of the first four PCs are presented in Fig.
 162 2, from which we clearly see that the accuracies of reconstructed PCs by our ISSA are
 163 obviously higher than those by SSAM, especially for the second and fourth PCs. In
 164 the case of 60% missing data, the accuracy improvements are up to 19.64, 41.34,
 165 23.27 and 50.30% for the first four PCs, respectively.

166



167
 168

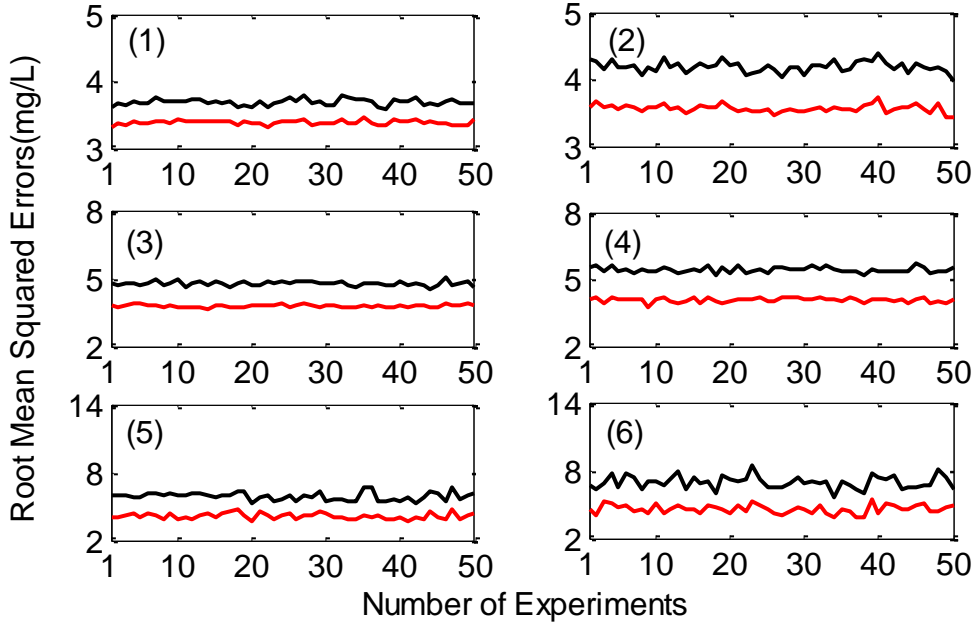
Figure 2. Relative errors of first four PCs (ISSA: red line; SSAM: black line)

169 We reconstruct the time series $\hat{c}(t)$ using the first four PC modes and then evaluate
 170 the quality of reconstructed series by examining the error $\Delta\hat{c}(t) = \hat{c}(t) - c_s(t)$. For the

171 cases whose missing data are between 10% to 50% over the whole time series, the
 172 reconstructed component of the time series is calculated only when the percentage of
 173 missing data in the window size is less than 50%; while for the cases whose overall
 174 missing data already reach 60%, it is allowed 60% missing data in the window size. In
 175 Fig. 3, we demonstrate the root mean squared errors (RMSE) of each experiment of
 176 different percentages of missing data. The RMSE is computed with $\Delta\hat{c}(t)$ as

$$177 \quad \text{RMS} = \sqrt{\sum_{j=1}^M \Delta\hat{c}^2(t_j)} / M \quad (19)$$

178 where M is the number of data points involved in the experiment.



179
 180 Figure 3. RMSE of 50 experiments, (1)~(6) represent percentage of missing data
 181 ranging from 10% to 60% with 10% increments.

182 As we can see from the Fig. 3, the RMSs of ISSA are much smaller than those of
 183 SSAM for all same experiment scenarios. In Table 1, we present the mean absolute
 184 reconstruction error (MARE) and mean root mean squared errors (MRMSE) of 50
 185 experiments with different percentages of missing data.

186 Table 1: Mean absolute reconstruction error and mean root mean squared error of
 187 simulated time series with different percentage of missing data (mg L^{-1})

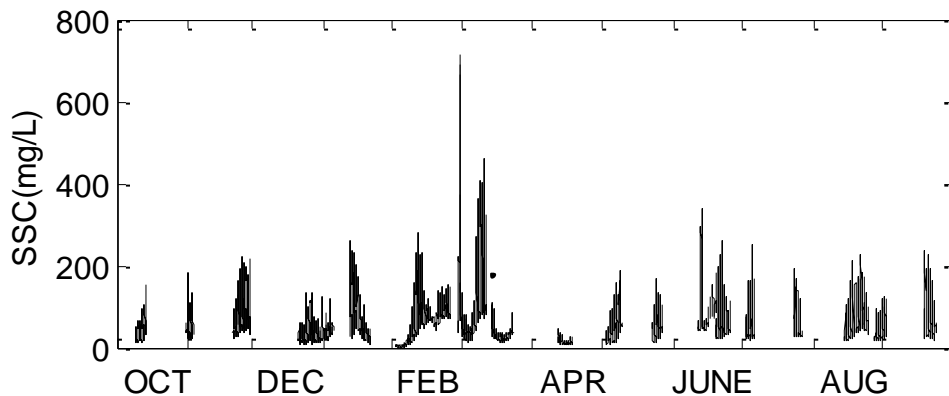
Percentage of Missing Data (%)	MARE			MRMSE		
	SSAM	ISSA	IMP (%)	SSAM	ISSA	IMP (%)
0	2.48	2.48	0	2.06	2.06	0%
10	2.87	2.60	9.41	3.68	3.38	2.21
20	3.26	2.73	16.26	4.19	3.56	15.04
30	3.71	2.90	21.83	4.76	3.78	20.59
40	4.22	3.11	26.30	5.42	4.07	24.91
50	4.57	3.17	30.63	5.89	4.14	29.71

60	5.37	3.52	34.45	6.96	4.60	33.91
SF Bay	3.38	3.08	8.87	2.70	2.29	15.19
Example						

188 Obviously, if there is no missing data, the ISSA coincides with SSAM. If the
189 percentage of missing data increases, both MARE and MRMSE will become larger.
190 In Table 1, all the MARE and MRMSE of ISSA are smaller than those of SSAM.
191 When the percentage of missing data reaches 50%, the MARE and MRMSE are
192 3.17 mg L^{-1} and 4.14 mg L^{-1} for ISSA, and 4.57 mg L^{-1} and 5.89 mg L^{-1} for SSAM,
193 respectively. The improved percentage (IMP) of ISSA with respect to SSAM is also
194 listed in Table 1. As the missing data increases, the IMPs of both MARE and
195 MRMSE increase as well. Moreover, when the synthetic time series with the missing
196 data is same as the real SSC time series of Fig. 4, the IMPs of MARE and MRMSE
197 are 8.87% and 15.19%, respectively.

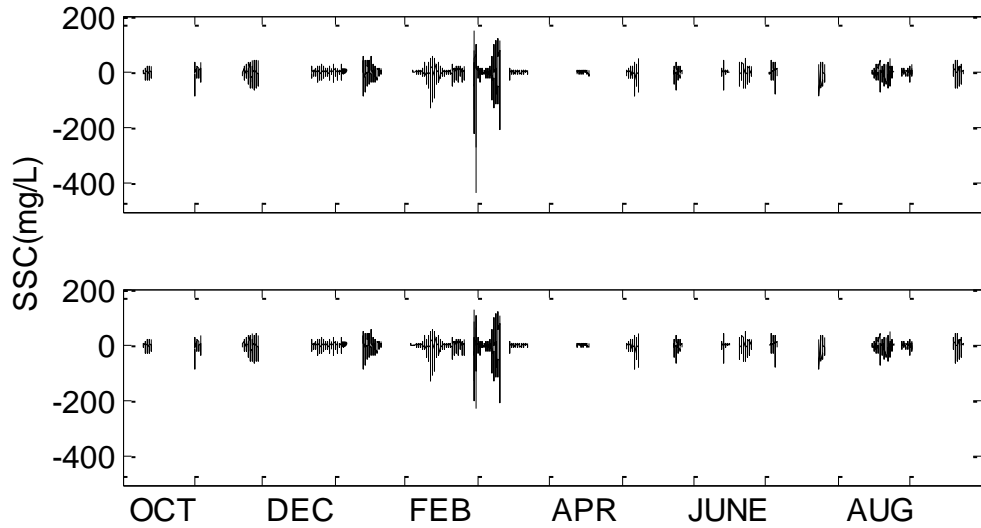
198 4. Performance of ISSA with real time series

199 The mid-depth SSC time series at San Mateo Bridge is presented in Fig. 4, which
200 contains about 61% missing data. This time series was reported by Buchanan and
201 Schoellhamer (1999) and Buchanan and Ruhl (2000), and analyzed by Schoellhamer
202 (2001) using SSAM. We analyze this time series using our ISSA with the window
203 size of 30h ($L=120$) comparing with SSAM. The first 10 modes represent dominant
204 periodic components as shown in Schoellhamer (2001) which contain 89.1% of the
205 total variance. Therefore, we reconstruct the time series with first 10 modes when the
206 missing data in a window size is less than 50%.



207
208 Figure 4. Mid-depth SSC time series at San Mateo Bridge during water year 1997

209 The residual time series, e.g. the differences of observed minus reconstructed data,
210 are presented in Fig. 5. The maximum, minimum and mean absolute residuals as
211 well as the SD are presented in Table 2. It is clear that both maximum and minimum
212 residuals are significantly reduced by using ISSA approach. The SD of our ISSA is
213 reduced by 8.6%. The squared correlation coefficients between the observations and
214 the reconstructed data from ISSA and SSAM are 0.9178 and 0.9046, respectively,
215 which reflect that the reconstructed time series with our ISSA can indeed, to very
216 large extent, specify the real time series.



217

218 Figure 5. Residual series after removing reconstructed signals from first 10 modes
 219 (top: SSAM; bottom: ISSA)

220 Table 2: Maximum, minimum and mean absolute residuals of SSAM and ISSA

Residuals(mg L ⁻¹)	SSAM	ISSA
Maximum	145.05	126.61
Minimum	-432.20	-227.70
Mean absolute residuals	8.19	8.00
SD	13.48	12.27

221

222

223

224 5. Conclusions

225 We have developed the ISSA approach in this paper for processing the incomplete
 226 time series by using the principle that a time series can be reproduced using its
 227 principal components. We prove that the SSAM developed by Schoellhamer (2001) is
 228 a special case of our ISSA. The performances of ISSA and SSAM are demonstrated
 229 with a synthetic time series, and the results show that the relative errors of the first
 230 four principal components by ISSA are significantly smaller than those by SSAM. As
 231 the fraction of missing data increases, the improvement of the relative error becomes
 232 greater. When the percentage of missing data reaches 60%, the improvements of the
 233 first four principal components are up to 19.64, 41.34, 23.27 and 50.30%, respectively.
 234 Moreover, when the missing data accounts for 60%, the MARE and MRMSE derived
 235 by ISSA are 3.52 mg L⁻¹ and 4.60 mg L⁻¹, and by SSAM are 5.37 mg L⁻¹ and 6.96 mg
 236 L⁻¹. The corresponding improvements of ISSA with respect to SSAM are 34.45 and
 237 33.91%. When the missing data of synthetic time series is the same as the real SSC
 238 time series, the improvements of MARE and MRMSE are 8.87 and 15.19%,
 239 respectively. The SD derived from the real SSC time series at San Mateo Bridge by
 240 ISSA and SSAM are 12.27 mg L⁻¹ and 13.48 mg L⁻¹, and the squared correlation
 241 coefficients between the observations and the reconstructed data from ISSA and

242 SSAM are 0.9178 and 0.9046, respectively. Therefore, ISSA can indeed, to a great
243 extent, retrieve the informative signals from the original incomplete time series.

244

245 **Author contribution**

246 Y. Shen proposes the improved singular spectrum analysis and F. Peng carries out the
247 FORTRAN program and performs the simulations. Y. Shen, F. Peng and B. Li prepare
248 the manuscript.

249

250 **Acknowledgements**

251 This work is sponsored by Natural Science Foundation of China (Projects: 41274035,
252 41474017) and partly supported by State Key Laboratory of Geodesy and Earth's
253 Dynamics (SKLGED2013-3-2-Z).

254

255 **References**

256 Broomhead, D.S., G.P. King, Extracting qualitative dynamics from experimental data.
257 *Physica D*, 20, 217-236, 1986.

258 Buchanan, P.A., and C.A Ruhl, Summary of suspended-solids concentration data, San
259 Francisco Bay, California, water year 1998, Open File Report 99-189, 41 pp.,
260 U.S. Geological Survey, 2000.

261 Buchanan, P.A., and D. H. Schoellhamer, Summary of suspended solids concentration
262 data, San Francisco Bay, California, water year 1997, Open File Report
263 00-88 URL <http://ca.water.usgs.gov/rep/ofr99189/>, 52 pp., U.S. Geological
264 Survey, 1999.

265 Golyandina, N., E. Osipov, The “Catterpillar”-SSA method for analysis of time series
266 with missing data, *J. Stat. Plan. Inf.*, 137, 2642-2653, 2007.

267 Hassani H., Mahmoudvand R., Zokaei M., et al. On the Separability between signal
268 and noise in singular spectrum analysis, *Fluct. Noise Lett.* 11(2), 1-11, 2012.

269 Hassani H., Mahmoudvand R. Multivariate singular spectrum analysis: a general view
270 and new vector forecasting approach, *Int. J. Energy Stat.*, 1(1), 55-83, 2013.

271 Kondrashov, D. M. Ghil, Spatio-temporal filling of missing points in geophysical data
272 sets, *Nonlin. Processes Geophys.*, 13, 151-159, 2006.

273 Oropeza, V., M. Sacchi, Simultaneous seismic data denoising and reconstruction via
274 multichannel singular spectrum analysis, *Geophysics*, 76(3), 25-32, 2011.

275 Robertson, A.W. and C. R. Mechoso, Interannual and decadal cycles in river flows of
276 southeastern South America, *Journal of Climate*, 11(10), 2570-2581, 1998.

277 Rodrigues, P.C., M. de Carvalho, Spectral modeling of time series with missing data,
278 2013

279 Schoellhamer, D.H., Factors affecting suspended-solids concentrations in South San
280 Francisco Bay, California, *J. Geophys. Res.*, 101(C5), 12087-12095, 1996.

281 Schoellhamer, D.H., Singular spectrum analysis for time series with missing data,
282 *Geophys. Res. Lett.* 28(16), 3187-3190, 2001.

283 Schoellhamer, D.H., Variability of suspended-sediment concentration at tidal to
284 annual time scales in San Francisco Bay, USA, *Continental Shelf Research*,
285 22, 1857-1866, 2002

286 Shen, Y., W. Li, G. Xu, B. Li. Spatiotemporal filtering of regional GNSS network's

287 position time series with missing data using principal component analysis,
288 Journal of Geodesy, DOI 10.1007/s00190-013-0663-y, Vol.88: 1-12, 2014
289 Vautard, R., P. Yiou, and M. Ghil, Singular-spectrum analysis: A toolkit for short,
290 noisy, chaotic signals, Physica D, 58, 95-126, 1992.
291 Vautard, R. and M. Ghil, Singular spectrum analysis in nonlinear dynamics with
292 applications to paleoclimatic time series, Physica D, 35, 395-424, 1989.
293 Wang, X.L., J. Corte-Real, and X. Zhang, Intraseasonal oscillations and associated
294 spatial-temporal structures of precipitation over China, J. Geophys. Res.,
295 101(D14), 19035-19042, 1996.
296 Yiou, P., K. Fuhrer, L.D. Meeker, J. Jouzel, S. Johnsen, and P.A. Mayewski,
297 Paleoclimatic variability inferred from the spectral analysis of Greenland
298 and Antarctic ice-core data, J. Geophys. Res., 102(C12), 26441-26454, 1997.
299 Zotova, L.V., C.K. Shum, Multichannel singular spectrum analysis of the gravity field
300 from grace satellites, AIP Conf. Proc., 1206, 473-479, 2010